

Supplementary Information

Electrosynthesis of Benzyl-tert-butylamine via Nickel-Catalyzed Oxidation of Benzyl Alcohol

P.J.L. Broersen, V. Paschalidou, A.C. Garcia*

Table of Contents

1.0 Calibration curves for HPLC analysis.....	2
2.0 Ni ⁰ oxidation to synthesize NiOOH (NiO ₂).....	4
3.0 Faradaic efficiency results at the three different applied potentials.....	5
4.0 Chronoamperometry for bulk electrolysis: benzyl alcohol oxidation in NaOH.....	6
5.0 Electrochemical Impedance Spectroscopy (EIS).....	7
6.0 Chronoamperometry for reductive amination.....	8
7.0 Fourier-Transform Infrared Spectroscopy (FTIR).....	9
8.0 Comparison with state of the art.....	10
References.....	11

1. Calibration curves for HPLC analysis

Liquid products were detected using high-performance liquid chromatography (HPLC). Figure S8 shows the calibration lines for the benzyl alcohol, benzaldehyde, benzoic acid and *tert*-butyl benzylamine. To construct the regression line, the products were mixed at known concentrations (1.8 mM, 0.36 mM, 0.18 mM and 0.0018 mM) with an internal standard solution of 1.6 mM furaldehyde. The area ratios of each of the 4 molecules with the internal standard were used to calculate the product concentration.

As explained in the main text, benzaldehyde reacts with *tert*-butylamine spontaneously at room temperature to form the intermediate imine. As a result, when the oxidation took place in the solution of 0.7 M *tert*-butylamine (pH = 11), some of the benzaldehyde would react away, deeming the calibration lines of the figure S6 inaccurate. For this reason, the calibration line shown at Figure S9 was constructed which is used only for the calculation of benzaldehyde in the conditions of the reductive amination (0.7 M *tert*-butylamine, pH = 11). To construct this calibration curve, benzaldehyde was dissolved at known concentrations (10 mM, 2 mM, 1 mM and 0.2 mM) in the *tert*-butylamine solution. The area of the aldehyde peak was plotted against the concentration of the benzaldehyde to calculate the product concentration.

For both calibration lines, analysis was done on an Agilent 1260 Infinity II system equipped with an Agilent Technologies Inc. Poroshell 120 EC-C18 column (150 x 3 mm, 2.7 μ m) and a RID and VWD detector. The column temperature was maintained at 35 °C. The mobile phase was acetonitrile/5 mM H₂SO₄, which was run in a gradient from 10/90 v/v to 80/20 after 25 min. at a flow rate of 0.5 mL min⁻¹.

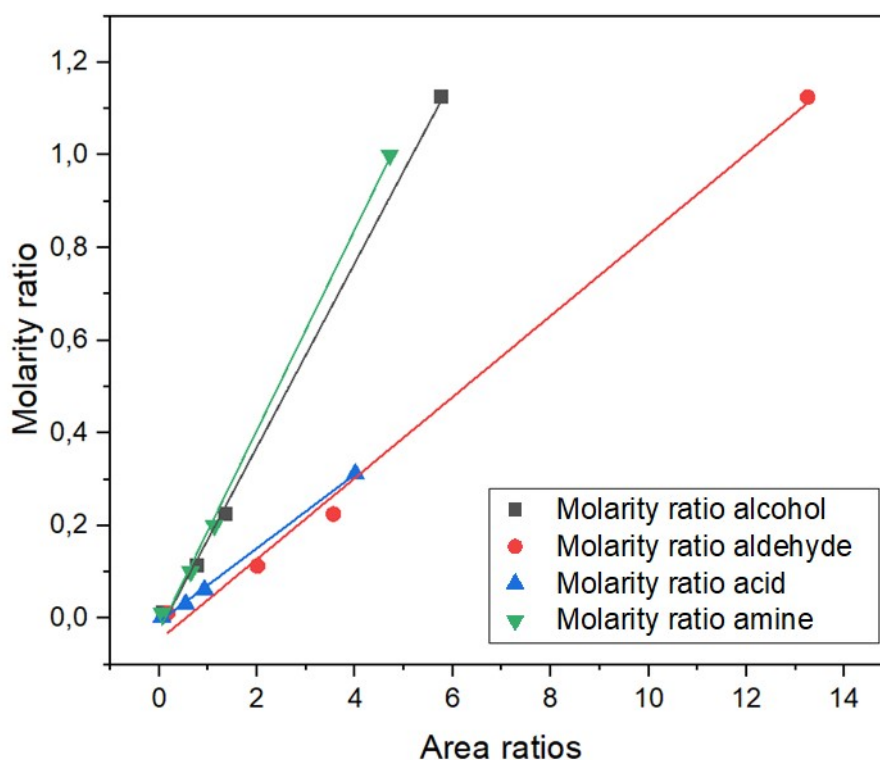


Figure S1. Calibration curves for benzyl alcohol, benzaldehyde, benzoic acid, and *tert*-butyl benzylamine. Benzyl alcohol: $R^2 = 0.999$, Equation = $-0.027 + 0.199x$. Benzaldehyde: $R^2 = 0.995$, Equation = $-0.047 + 0.0875x$. Benzoic acid: $R^2 = 0.999$, Equation = $-0.0078 + 0.0796x$. Benzyl-*tert*-butylamine: $R^2 = 0.998$, Equation = $-0.027 + 0.217x$.

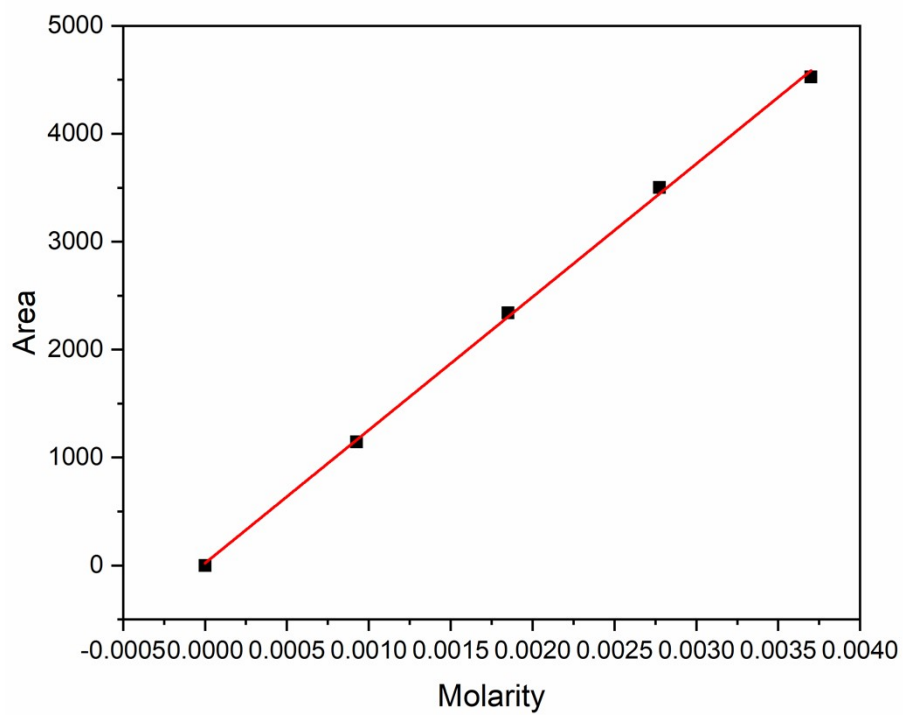


Figure S2. Calibration curve for benzaldehyde concentration in a solution of 0,7 M *tert*-butylamine pH = 11. $R^2 = 0.999$; Equation: $y = 20 + 1.23x$.

2. Ni^0 oxidation to synthesize NiOOH (NiO_2)

To synthesize the NiOOH electrode, we oxidized Ni^0 by cycling 20 times from 1.0 V to 1.81 V vs RHE until it stabilized (last scan shown in Figure S1).

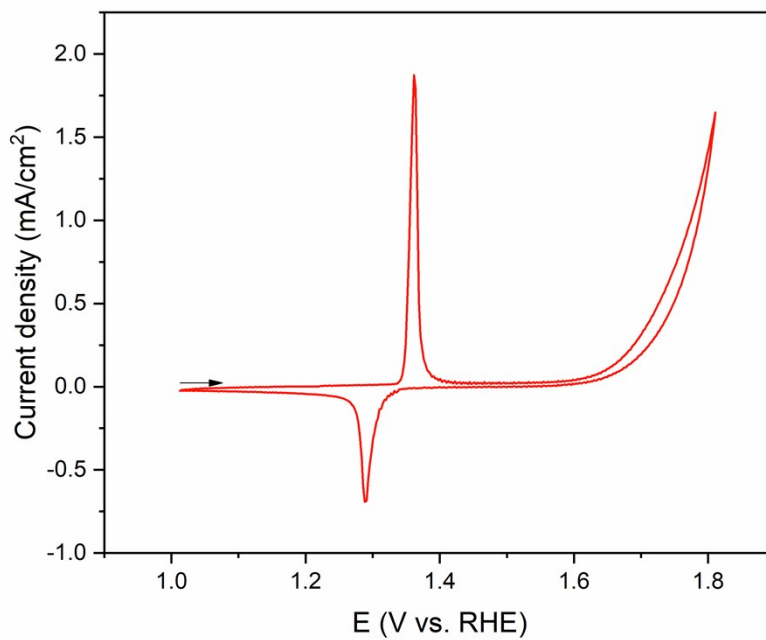


Figure S3. 20th cycle of Ni^0 oxidation of 2 equivalent monolayers. Arrow indicates the direction of the scan. Scan rate = 50 mV s^{-1} .

3. Faradaic efficiency results at the three different applied potentials

As a first step of the deconvolution of the benzyl alcohol oxidation reaction, we investigated which potential leads to higher selectivity towards benzaldehyde. After performing a CV (Figure 1B) and identifying the three peaks of interests, we performed bulk electrolysis for the three different points. HPLC analysis revealed that at potential 1.58 vs RHE, the faradaic efficiency towards benzaldehyde was the biggest.

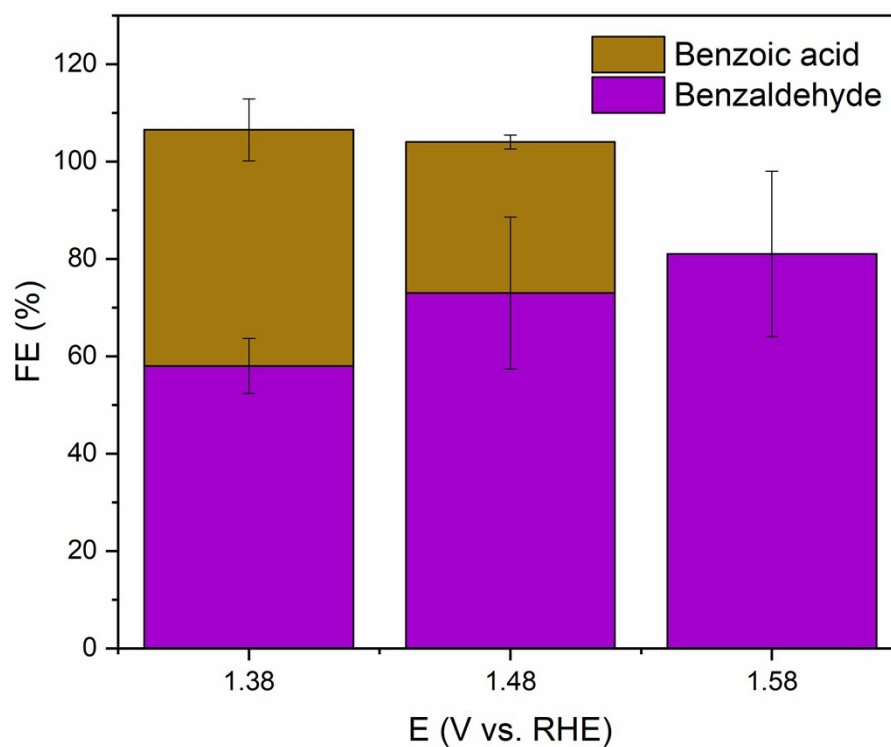


Figure S4. Comparison of the faradaic efficiencies towards benzaldehyde and benzoic acid at 3 different potentials. 5 NiOOH monolayer equivalents were used for the bulk electrolysis experiments.

4. Chronoamperometry for bulk electrolysis: benzyl alcohol oxidation in NaOH

Chronoamperometry for benzyl alcohol oxidation in a divided cell 1.0 M NaOH, 30 mL reaction volume. The current density decreased with time as the NiOOH catalyst leached into the solution or active sites are blocked by alcohol oxidation products, thus lowering the number of active sites.

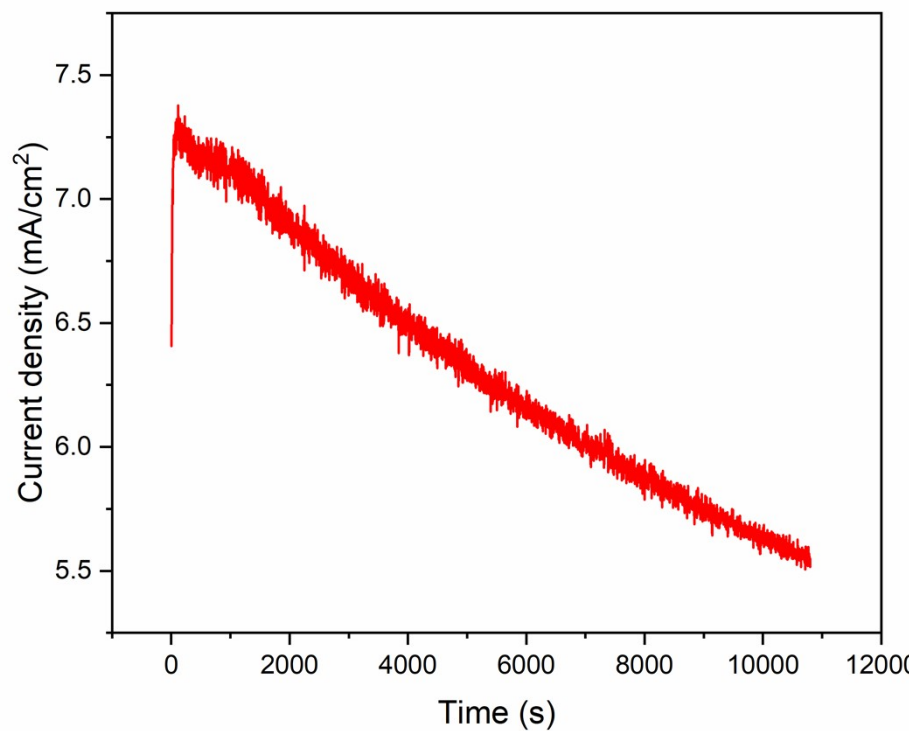


Figure S5. Chronoamperometry of benzyl alcohol oxidation with 2 NiOOH monolayer equivalents. 1.48 V vs RHE for 3 hours

5. Electrochemical Impedance Spectroscopy (EIS)

Impedance spectroscopy was used to analyze the surface area of the nickel catalyst. This was done through the calculation of the roughness factor. First, we electrodeposited and synthesized 2 and 10 monolayer equivalents on a gold electrode ($\phi = 5$ mm) with the process mentioned in the experimental section of the main text. After we characterized and confirmed the number of monolayers, the electrode was transferred to a 0.1 M purified NaOH solution. EIS was performed at 1.6 V vs RHE, where the NiOOH had fully formed but OER did not yet occur. From the data from the Nyquist the roughness factor was calculated by fitting the data to an Armstrong-Henderson equivalent circuit. The double layer capacitance was calculated from the equation:

$$C_i = \left(\frac{C'_i}{(R_{el}^{-1} + R_i^{-1})^{1-n_i}} \right)^{1/n_i}$$

where R_i is either R_{ct} or R_{ads} for C_i being C_{dl} or C_{ads} , respectively. The double layer capacitance was calculated to be $11 \mu\text{F}/\text{cm}^2$ and $296 \mu\text{F}/\text{cm}^2$ for the 2 and 10 NiOOH monolayers respectively. The results support the theory that the 10 monolayers have nearly 30 times higher surface area, meaning the it is more likely that the catalysts are forming porous channels (Figure 3 main text), thereby trapping the formed benzaldehyde, promoting overoxidation.

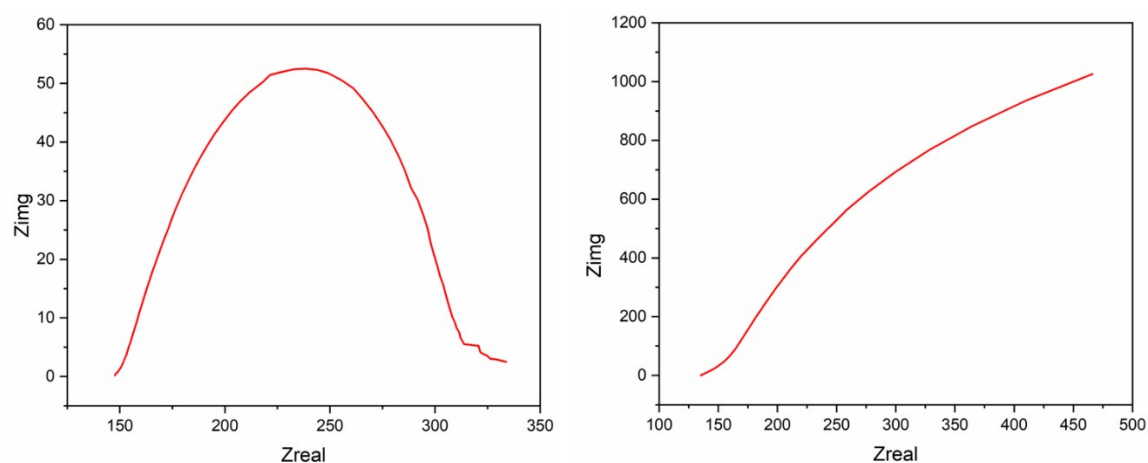


Figure S6. EIS Nyquist plot for the 2 (LEFT) and 10 (RIGHT) monolayer equivalents

6. Chronoamperometry for reductive amination

Below, a chronoamperometry graph is shown for a typical benzaldehyde reductive amination experiment. The bulk electrolysis was performed in a divided cell with 10 mL working solution, separated by a Nafion 117 proton-exchange membrane. The current density decreased over time, likely as the *tert*-butylamine covers the surface area of the Ag electrode, slightly inhibiting the reduction reaction. Graphite was used as counter electrode and RHE as reference electrode.

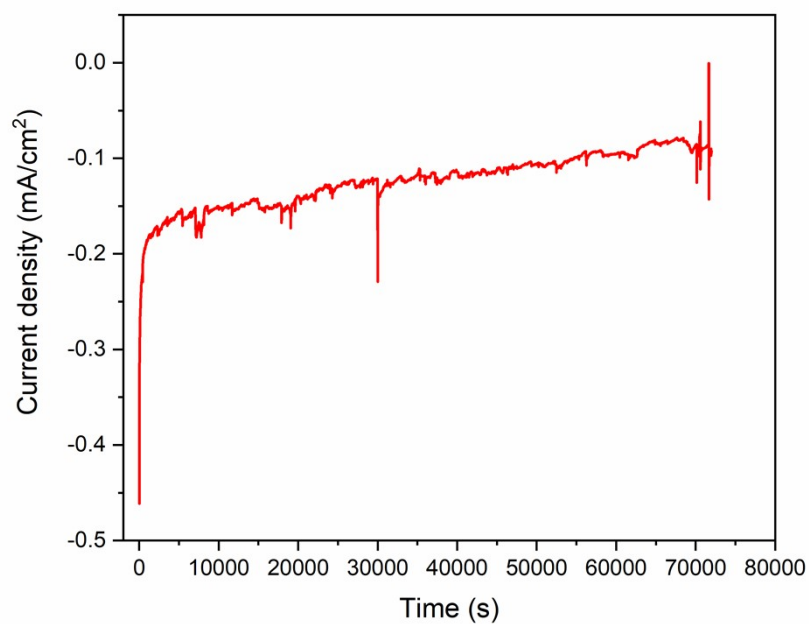


Figure S7. Reductive amination of benzaldehyde 0.02 M for 20 h using an Ag disk as electrode.

7. Fourier-Transform Infrared Spectroscopy (FTIR)

As part of the mechanistic studies of the reaction, FTIR experiments in NaOH and in *tert*-butylamine (main text) were conducted and the results were compared. 0.1 M of benzyl alcohol and 1.0 M NaOH were used. In the figure below we identified the production band at 1388 cm^{-1} as the stretching of the C–O bond of the benzaldehyde. Additionally, the peak at 1544 cm^{-1} we identified as the band corresponding to the asymmetric stretching of the O–C–O bond of the benzoic acid.^[27] Both peaks appear after 1.45 V, meaning that they are the result of the catalytic activity of NiOOH. As the potential increases, the oxygen evolution reaction also increases which could explain the shift of the consumption band from 3080 to 2700 cm^{-1} .

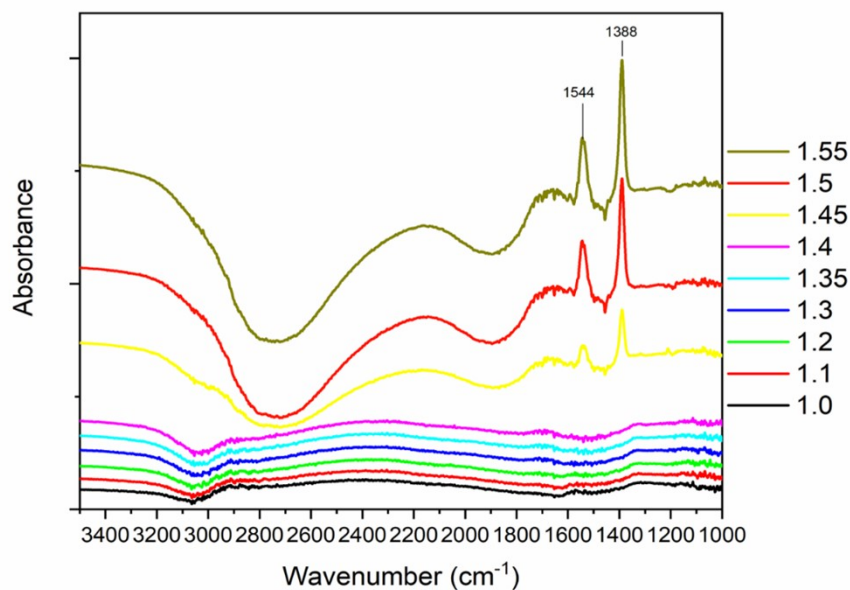


Figure S8. FTIR spectrum of benzyl alcohol oxidation in NaOH at different potentials vs RHE. 10 monolayer equivalents of NiOOH were used.

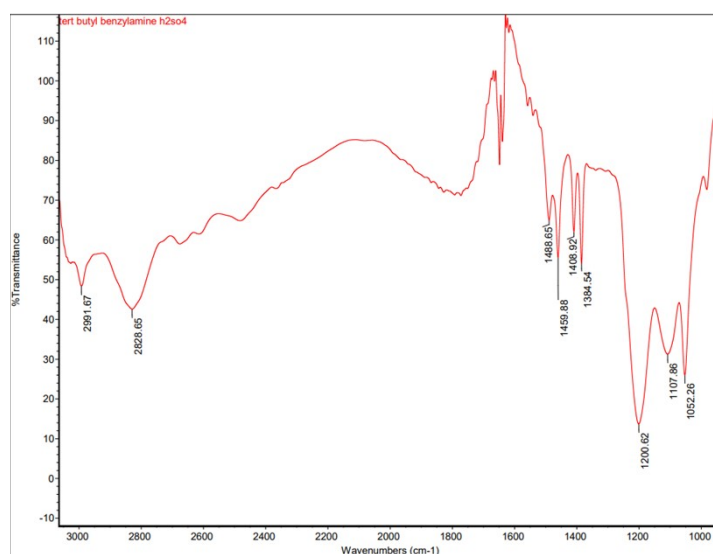


Figure S9. Transmission FTIR spectrum of a 0.1 M benzyl-*tert*-butylamine solution in 0.7 M *tert*-butylamine acidified to pH 11.0 with H_2SO_4 .

8. Comparison with state of the art

Table S1 compares our results to the current state of the art in hydrogen borrowing catalysis, to show how it improves the sustainability of the alcohol to amine conversion process, based on reaction conditions, solvent choice, metal use etc. What can be seen from this comparison is that the solvent choice is greener, since our reaction is performed in water. The lower temperature and pressure are also desirable. What may be the greatest benefit of our work is that the materials that are used for the catalysis are cheaper than the platinum, iridium and ruthenium-based ones that are often used in hydrogen borrowing catalysis, and are also more earth abundant.

Table S1: Comparison of state of the art hydrogen borrowing catalysis with our work.

Catalyst	Solvent	Temperature	Pressure	Ref
NiOOH/Ag	H ₂ O	RT	Atm.	This work
Ni nanoparticle	Cyclopentyl methyl ether	140 °C	Atm.	[1]
Ru(L)	Cyclohexane	140 °C	unspecified	[2]
Ru/TiO ₂	Toluene	110 °C	7 bar	[3]
Ir(CPA)	Toluene	90 °C	Atm.	[4]
Pt/CeO ₂	Neat	80 °C	10 bar	[5]
RaneyNi®	<i>t</i> -amyl alcohol	120 °C	>7 bar	[6]
Ru(<i>p</i> -cymene)Cl ₂	Neat	150 °C	50 bar	[7]
Fe(L)	Toluene	130 °C	unspecified	[8]
Ir(L)	Toluene	110 °C	Atm.	[9]
Ru/ACC	H ₂ O/alcohol	60 °C	Atm.	[10]

References

- [1] A. Afanasenko, S. Elangovan, M. C. A. Stuart, G. Bonura, F. Frusteri, K. Barta, *Catal. Sci. Technol.* **2018**, *8*, 5498–5505.
- [2] D. Pingen, O. Diebolt, D. Vogt, *ChemCatChem* **2013**, *5*, 2905–2912.
- [3] Y. Kita, M. Kuwabara, S. Yamadera, K. Kamata, M. Hara, *Chem. Sci.* **2020**, *11*, 9884–9890.
- [4] Y. Liu, P. Ji, G. Zou, Y. Liu, B.-M. Yang, Y. Zhao, *Angew. Chemie Int. Ed.* **2024**, e202410351.
- [5] S. Jia, T. Tong, X. Liu, Y. Guo, L. Dong, Z. Chen, Y. Wang, *J. Catal.* **2024**, *432*, 115407.
- [6] X. Wu, M. De Bruyn, K. Barta, *Catal. Sci. Technol.* **2022**, *12*, 5908–5916.
- [7] R. Labes, C. Mateos, C. Battilocchio, Y. Chen, P. Dingwall, G. R. Cumming, J. A. Rincón, M. J. Nieves-Remacha, S. V. Ley, *Green Chem.* **2019**, *21*, 59–63.
- [8] X. Bai, F. Aiolfi, M. Cettolin, U. Piarulli, A. Dal Corso, L. Pignataro, C. Gennari, *Synthesis.* **2019**, *51*, 3545–3555.
- [9] X. Xi, Y. Li, G. Wang, G. Xu, L. Shang, Y. Zhang, L. Xia, *Org. Biomol. Chem.* **2019**, *17*, 7651–7654.
- [10] B. Appiagyei, S. Bhatia, G. L. Keeney, T. Dolmetsch, J. E. Jackson, *Green Chem.* **2020**, *22*, 860–869.